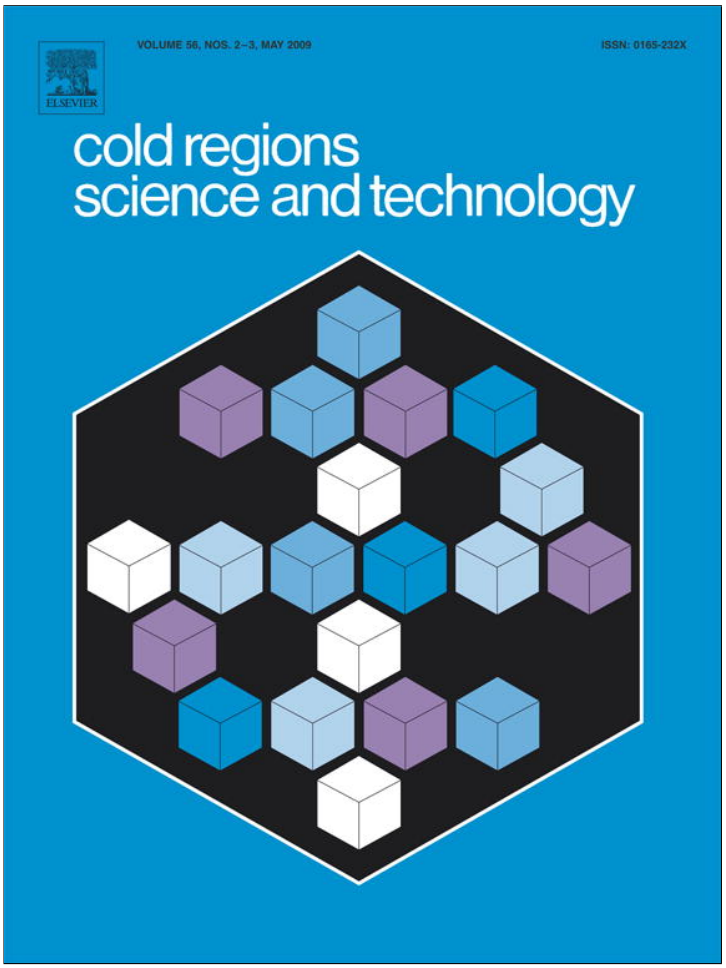

Cold Regions Science and Technology 56 (2009) 98–101

Contents lists available at ScienceDirect

Cold Regions Science and Technology

journal homepage: www.elsevier.com/locate/coldregions

Sea ice thickness measurement using episodic infragravity waves from distant storms

Peter Wadhams [a,b], Martin J. Doble [b,*]

[a] Université Pierre et Marie Curie—Paris VI, LOV, 06234 Villefranche-sur-Mer, France
[b] Department of Applied Mathematics and Theoretical Physics, University of Cambridge, Cambridge CB3 0WA, UK

ARTICLE INFO

Article history:
Received 27 November 2008
Accepted 11 December 2008

Keywords:
Sea ice
Thickness
Waves

ABSTRACT

The thinning and retreat of Arctic sea ice is one of the most dramatic manifestations of recent climate warming. Though ice extent can be routinely monitored by satellite, ice thickness is far more difficult to measure operationally. We show that small amplitude, long period waves — termed infragravity waves — can be used to measure ice thickness at basin scales by determining their travel time between measurement sites. The waves travel at a different speed in ice than in open water, the difference being a sensitive function of ice thickness. We present measurements from near the North Pole where the travel time of 15 s waves is reduced by around 7 h for a typical 2 m ice thickness. Our results demonstrate that a basin-scale observation network which can track the effect of global change on Arctic sea ice thickness is practical and feasible using current technology.

1. Introduction

Ocean surface waves which approach the Arctic pack ice first encounter the marginal ice zone (MIZ) of broken floes, where higher frequency components (less than 15 s period) are attenuated by scattering within a few tens of km (Wadhams et al., 1988). Longer period waves survive to reach the more continuous interior ice, where they continue to propagate as low-amplitude (of order mm) flexural-gravity waves with a slightly different dispersion relation from open-ocean waves. Measurement of these waves is relatively straightforward, using accelerometers or gravimeters to sense the heave of the ice, or tiltmeters or strainmeters to determine the flexing of the ice membrane, and the resulting spectra show typical peak periods of 15–30 s.

Ocean waves of such long periods are termed infragravity waves, and are believed to be generated in shallow water by non-linear interactions between storm-generated swell waves of approximately 15 s period (Herbers et al., 1995; Longuet-Higgins and Stewart, 1962). These long waves have been seen in records from ocean bottom seismometers (OBSs) and have been identified as responsible for the Earth's background seismic "hum" (Webb, 2007). They propagate in the deep ocean without significant further attenuation (Lighthill, 1978). Observations from OBSs do not represent the full spectrum of infragravity waves, since the pressure signal at the seafloor decays exponentially with the product of wave number and water depth (Webb et al., 1991). Spectra from OBSs typically exhibit a "noise notch" between 0.03 Hz and 0.1 Hz, due to this process — often termed "hydrodynamic filtering". Measurements on sea ice may therefore represent the most accurate and practical means of detecting and describing the infragravity wave spectrum.

Wave measurement in the interior of the Arctic Ocean began in the 1950s (Crary et al., 1952; LeShack and Haubrich, 1964) and continued during ice physics campaigns such as FRAM-II and -III, CEAREX, AIWEX and SIMI. The dispersive properties of a wave which propagates partly in the water column and partly by causing the ice sheet to flex elastically were first derived by Greenhill (1887) and experimentally confirmed by Ewing and Crary (1934). The slow decay of such waves in ice was ascribed to creep losses incurred in ice flexure, a thickness-dependent process which offers a method of deriving mean ice thickness by measuring attenuation along the wave propagation path (Menemenlis et al., 1995; Wadhams, 1973; Wadhams, 1986). It was later suggested that the ice cover 'selects' a preferred "resonant" frequency, at which a wave travels at the same speed in the ice as in the water, and that observations of this resonant wave might be used to infer path-integrated ice thickness without reference to mechanical parameters (Johannessen et al., 2004; Nagurny et al., 1999; Nagurny et al., 1994), although no mechanism for such a selection process was proposed.

We have developed and deployed a series of autonomous wave measuring buoys at locations across the Arctic, as part of the European Union GreenICE (Greenland Arctic Shelf Ice and Climate Experiment) project to investigate in detail the nature of long wave propagation and decay in the ice. The system was described in Doble et al. (2006), and essentially consists of two orthogonal tilt sensors which record time series of ice tilt and report over the *Iridium* satellite system. Results from the GreenICE deployments — in the Lincoln Sea north of Greenland and Canada's Ellesmere Island (Haas et al., 2006) — proved difficult to interpret, since the surrounding shallow bathymetry (Morris Jesup Rise, Lomonosov Ridge, Greenland continental

* Corresponding author.
E-mail address: M.J.Doble@damtp.cam.ac.uk (M.J. Doble).

0165-232X/$ – see front matter © 2009 Elsevier B.V. All rights reserved.
doi:10.1016/j.coldregions.2008.12.002

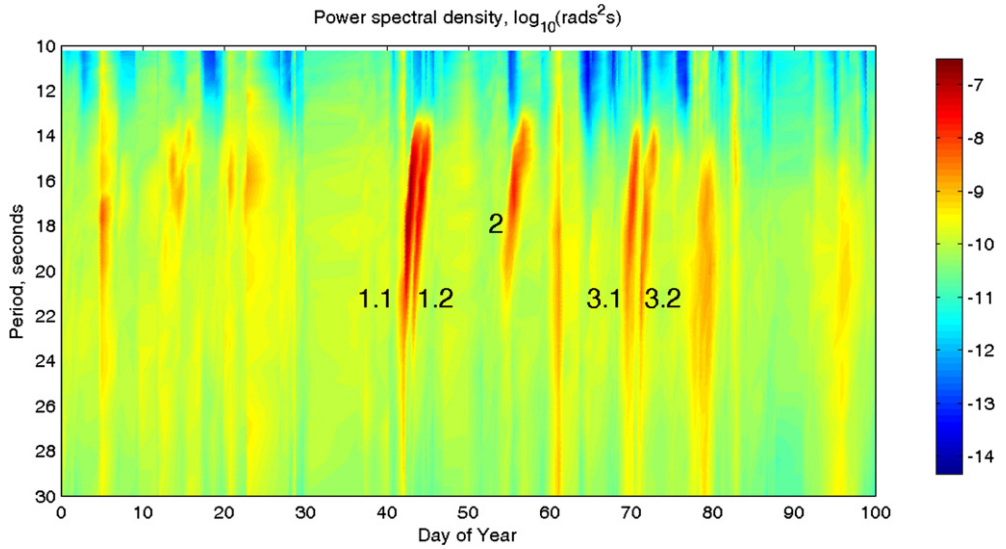

Fig. 1. The tiltmeter record for the first 100 days of 2007, with invalid records (contaminated with floe collisions etc) removed. The graph shows a contour plot of the spectral power in one tiltmeter channel, with the colour scale showing $\log_{10}(\text{rads}^2\text{s})$. Three events stand out with significantly higher power and these correspond to clear swell peaks in the spectra. Event numbers are labelled on the graph and referred to in the text. (For interpretation of the references to colour in this figure legend, the reader is referred to the web version of this article.)

shelf) refract and reflect the long-period (hence long wavelength) waves of interest. Evidence from these deployments strongly suggested that the waves were arriving from lower-latitude oceans, however, and an uninterrupted deep-water ray path to the measurement site was sought for further deployments.

The European Union DAMOCLES project provided such an opportunity and Doble deployed a tiltmeter alongside the schooner *Tara* at the beginning of its two year drift across the Arctic (Gascard et al., 2008), in September 2006, at 79°51′N 143°32′E. The manned *Tara* station allowed the unit to be configured to record continuously, writing three-hour time series files to CompactFlash card. We present data spanning the first 100 days of 2007, during which time the drifting station was between 85°N and 87°N, heading slowly towards the North Pole along longitude 130°E, just to the west of the Lomonosov Ridge. The location offered an essentially clear deep-water path to waves arriving from lower-latitude seas, through the narrow deep-water aperture of Fram Strait, between Greenland and Svalbard.

2. Results

2.1. Dispersive arrivals

Each three-hour tilt time series was first bandpass filtered (10 to 60 s period) to remove secular drift, DC components and higher frequency noise. Spectra were calculated using the Welch method of overlapping segments to give the lowest variance per data point (Emery and Thomson, 1998), then examined individually to eliminate records contaminated by excessive floe–floe collisions, characterised by impulsive, high-amplitude events which tended to mask the wave signal. Remaining values (197 cases) are displayed in Fig. 1. Sharply peaked spectra are associated with high spectral power, more than two orders of magnitude above the background level.

Three events, separated by around two weeks, are particularly prominent. The first and last events display two closely separated arrivals, marked as Events 1.1, 1.2 and 3.1, 3.2 in Fig. 1. The events have an increasing peak frequency with time. First arrivals have a frequency around 0.03 Hz, increasing to around 0.07 Hz before the spectral power drops to near background level. The plot recalls the dispersive character of waves arriving from distant storm events, examined in the "waves across the Pacific" series of experiments (Munk and Snodgrass, 1957) and we use the relation given in those works to calculate the distance implied by the observed frequency–time relation here:

$$x = \frac{g}{4\pi f}(t - t_0) \tag{1}$$

where x is the distance to the source, g is the acceleration due to gravity, f is the observed peak frequency, t the time of the observation and t_0 the time of emission of the waves (calculated as the time that the fitted line crosses the zero-frequency axis). We assume deep water ($kH \gg 1$), a stationary source region and that waves of all frequencies are generated simultaneously in a given storm event.

The group velocity of waves travelling in ice depends on both the frequency and the ice thickness, but for realistic thicknesses (e.g. 2 m) the speeds are only significantly different from those in open water at periods less than around 20 s. Fig. 2 compares the group velocity of

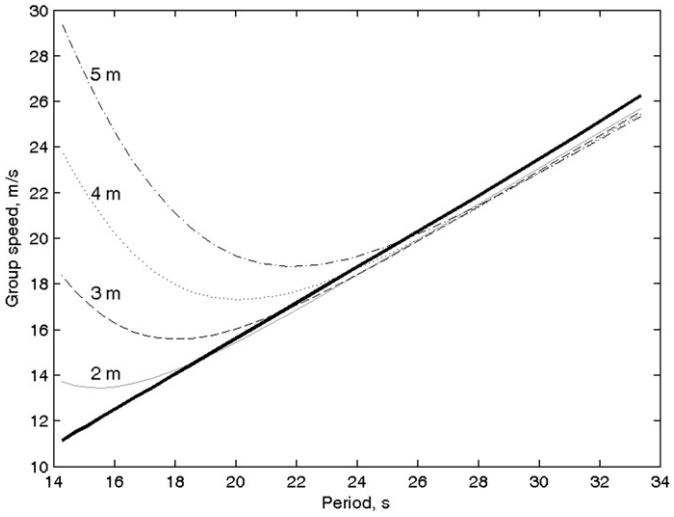

Fig. 2. Group velocity *versus* period for open water (heavy line) and ice thicknesses from 2–5 m, showing the increased velocity in ice with shorter period.

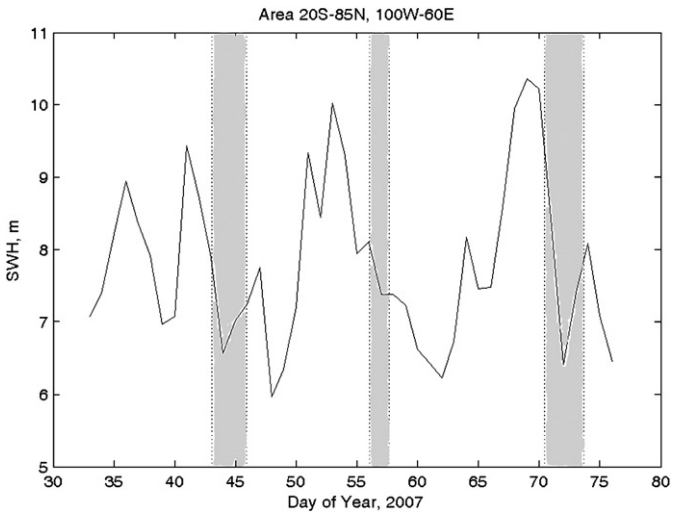

Fig. 3. Maximum significant waveheight observed by the JASON satellite altimeter in the North Atlantic (20S–85N, 100W–60E). The duration of the peak events measured by the tiltmeter are indicated as shaded regions, following each maximum SWH.

waves in open water to that in ice of various thicknesses, using the dispersion relation (Eq. 14.13 of Wadhams, 1986), solved numerically:

$$Dk_0^5 + \left(\rho_w g - \rho_i h\omega^2\right)k_0 - \rho_w\omega^2 = 0 \quad (2)$$

$$D = Eh^3 / 12\left(1 - \nu^2\right) \quad (3)$$

Where k_0 is wavenumber, ρ_w and ρ_i the densities of water and ice, respectively, h the ice thickness and ω the wave angular frequency. D is termed the flexural rigidity and depends on the Young's modulus (E) and Poisson's ratio, ν. Here we have taken $\rho_w = 1025$ kg m^{-3}, $\rho_i = 900$ kg m^{-3}, $E = 6\times10^9$ Pa, $\nu = 0.3$.

At the longest periods observed, the group velocity in ice is slightly less than in open water. As the period drops, group velocity in ice becomes significantly greater than in open water, the effect increasing with ice thickness and being due to the influence of the flexure on the overall propagation. Waves in the 20–30 s period range can be validly assumed to lie close to the open water relation and these were used to establish the source distance, while the shorter waves are used for the thickness derivation.

2.2. Source location

The frequency–time relations gave source locations between 6300 and 9700 km from the measurement site. These are large distances, equivalent to between 60° and 90° of latitude, precluding generation within the Arctic Basin itself and implying a source within the North Atlantic. We expect the wave sources to be of northern hemisphere origin, since the long period waves are most prominent in the northern hemisphere winter (Doble et al., 2006).

We identified the source events by examining global daily significant wave height (SWH) data from the JASON satellite altimeter (http://www.aviso.oceanobs.com). Global maps clearly indicated the North Atlantic as the likely source region, with very few high-amplitude events occurring during these periods in the rest of the world ocean. SWH observed in this Atlantic sector (20°S to 85°N and 100°W to 60°E) during the period of interest (Fig. 3) showed three clear maxima, each preceding the observed dispersive arrival events by two or three days, though ranges to these storm centres were 20–50% lower than those calculated from Eq. (1).

The bathymetry between the measurement site and the mid-latitude North Atlantic is rather complex, with Fram Strait, Denmark Strait and the Faeroes-Shetland Channel offering the only deep-water paths (>500 m) for the passage of the long waves in question. Also, infragravity waves are not generated directly at the storm site: recent observations have shown that storm waves must first to travel to a sloping sandy coastline for the non-linear interaction to occur (Dolenc et al., 2008) and previous studies of infragravity waves selected such sloping beaches as study sites (Elgar et al., 1992; Henderson et al., 2006). The location of interest is therefore that of the infragravity wave generation site, not the storm itself. A Great Circle path from *Tara* through Fram Strait intersects the northwest African coast at the approximately the ranges calculated from the $f(t)$ relation. This location is therefore tentatively suggested as the source, though interaction with bathymetry (refraction) may deviate waves arriving from other sources onto the required track, for instance during passage through the Faeroes-Shetland Channel, northwest of the United Kingdom. The closely separated arrivals measured for events 1 and 3 suggest two slightly differing paths to *Tara*.

2.3. The effect of the ice cover

Wherever the infragravity waves are generated, they must pass through the deep channel of Fram Strait and then travel a significant distance though the pack ice to reach the measurement site. Such an extended path in ice suggests that even small changes in group velocity should result in measurable perturbations to the waves' travel time. The path length in ice for the current example varies between 1514 and 1630 km, measured from passive microwave satellite imagery supplied by the Danish Meteorological Institute.

Fig. 4 plots the expected reduction in travel time due to this ice, for the frequency range of the observed dispersive events and various ice thicknesses. Data collected by upward-looking sonar from the submarine HMS *Tireless* during the period of these observations (March 2007) cover about 40% of the wave path, and give a path-averaged modal ice thickness of about 2.1 m (Wadhams, unpublished data) which is marked on the plot. For a uniform ice cover of this thickness, the lowest frequencies (0.035 Hz) arrive around 20 min after their open water equivalents, while the highest frequencies (0.07 Hz) arrive around seven hours before. Travel time is thus modified by a significant amount, easily measurable with current technology, and is a sensitive function of both ice thickness and frequency. The technique thus allows ice thickness along the wave path to be remotely sensed.

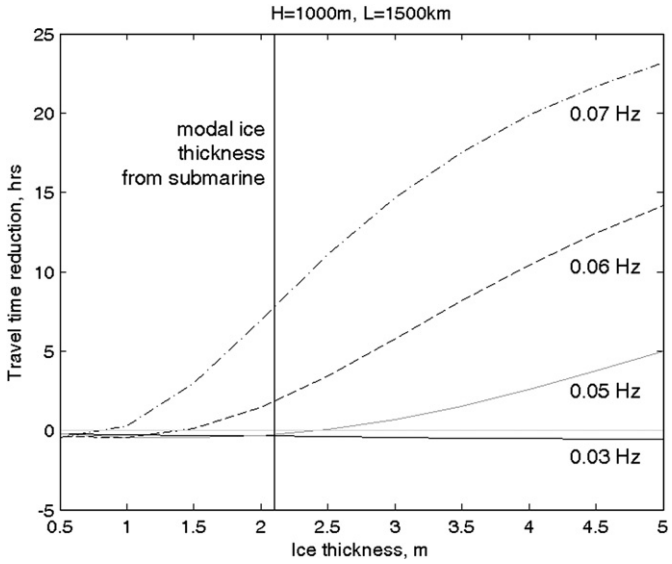

Fig. 4. Travel time reduction, compared to open water propagation, at the measurement site, plotted as a function of ice thickness, for several frequencies within the observed range. Path length in ice is set to 1500 km. The modal ice thickness value obtained from concurrent submarine upward-looking sonar measurements is marked.

3. Discussion

We have seen that the nature of infragravity wave generation makes it difficult to determine where or when the waves originated, even if the location and timing of the storm which generated the shorter waves are known. This does not prevent application of our method to ice thickness measurement, since only the perturbation due to the waves' passage through the ice is relevant. Two tiltmeters, widely separated along the wave path, will allow measurement of the modal ice thickness between instruments: once a dispersive wave train has been identified, we simply measure the time that any convenient frequency takes to travel between instruments and compare this with the open water travel time at the same frequency. The exact arrival time of a given frequency within a three-hour time series is derived from wavelet analysis. It is not necessary to determine when the amplitude of the waves first begins to increase above background levels.

The high energy levels of shorter waves close to the ice edge may obscure the much lower amplitude infragravity waves there, but multiple tiltmeter instruments, located at increasing penetrations into the ice cover, should resolve arrivals from distant storms with sufficient accuracy to allow a reasonable estimation of the ice thickness. Results presented here have shown that measurement is feasible for the region between Fram Strait and the central Arctic, where a relatively direct deep-water path exists. A basin-scale ice thickness measuring array is therefore proposed. Instruments will need to record continuously and — to limit satellite transmission costs — be able to identify a train of dispersive arrivals. Once flagged as "interesting" by onboard signal processing, stored time series would then be transmitted for more detailed analysis at the laboratory. Such refinements represent only minor changes to the existing hardware and software.

We expect the technique to measure the path-integrated modal ice thickness, since ice thickness will affect the travel time as a linear relation to its fraction in the probability density function of thickness. The mode is typically the thickness of the most common type of undeformed ice present, which in the central Basin is more often first-year than multi-year ice. For validation purposes, initial measurements should ideally be taken concurrently with submarine ice draft profiles along the same path. Such measurements will also allow a representative value of Young's modulus to be obtained, which is a free parameter in the dispersion relation. A value of 6×10^9 Pa has been used here, following Wadhams (1986), but , but its applicability to large-scale sea ice bending applications is largely unknown, whilst higher values of 7–9.5 Pa have been quoted for small-scale deformation (Sanderson, 1988).

The results presented here have demonstrated that more than 1000 km of sea ice cover does not significantly attenuate such long period waves: frequencies from 0.03 Hz to 0.07 Hz were clearly measured at the *Tara* site with significant amplitudes. No evidence of a "resonant" wave was found; all long periods appear to be present and the peak frequency is determined by travel time from the distant storm. Thus the Arctic Ocean offers a natural laboratory for isolating and studying infragravity waves, while the dispersive properties of the waves in ice offer a means of monitoring modal ice thickness over much of the Arctic, of great importance at a time when the ice is thinning and retreating so rapidly, since it is the preferred thickness of undeformed ice (mode) which determines whether the ice cover will melt during the enhanced summer warming now being experienced.

Acknowledgements

The work was funded by the DAMOCLES project, grant no. 018509 of the European Union 6th Framework Program. We gratefully acknowledge the assistance of the crew of *Tara* — particularly Hervé le Goff, Jean Festy and Matthieu Weber — for maintaining the instrumentation. The travel time perturbation approach to measuring ice thickness was first suggested to us by Walter Munk, to whom we are grateful for valuable discussions.

References

Crary, A.P., Cotell, R.D., Oliver, J., 1952. Geophysical studies in the Beaufort Sea. EOS Trans. AGU 33 (2), 211–216.
Doble, M.J., Mercer, D., Meldrum, D., 2006. Wave measurements on sea ice: developments in instrumentation. Ann. Glaciol. 44, 108–112.
Dolenc, D., Romanowicz, B., McGill, P., Wilcock, W., 2008. Observations of infragravity waves at the ocean-bottom broadband seismic stations Endeavour (KEBB) and Explorer (KXBB). Geochem. Geophys. Geosystems 9 (5). doi:10.1029/2008GC001942.
Elgar, S., Herbers, T.H.C., Okihiro, M., Oltman-Shay, J., Guza, R.T., 1992. Observations of infragravity waves. J. Geophys. Res. 97 (C10), 15573–15577.
Emery, W.J., Thomson, R.E., 1998. Data Analysis Methods in Physical Oceanography. Pergamon, Oxford. 634 pp.
Ewing, M., Crary, A.P., 1934. Physics 5, 181.
Gascard, J.C., Festy, J., le Goff, H., Weber, M., Bruemmer, B., Offermann, M., Doble, M., Wadhams, P., Forsberg, R., Hanson, S., Skourup, H., Gerland, S., Nicolaus, M., Metaxian, J.P., Grangeon, J., Haapala, J., Rinne, E., Haas, C., Heygster, G., Jakobson, E., Palo, T., Wilkinson, J., Kaleschke, L., Claffey, K., Elder, B., Bottenheim, J., 2008. Exploring Arctic transpolar drift during dramatic sea ice retreat. Eos, Trans. Amer. Geophys. U. 89 (3), 21–28.
Greenhill, A.G., 1887. Wave motion in hydrodynamics. Am. J. Math. 9 (62–112).
Haas, C., Hendriks, S., Doble, M.J., 2006. Comparison of the sea ice thickness distribution in the Lincoln Sea and adjacent Arctic Ocean in 2004 and 2005. Ann. Glaciol. 44.
Henderson, S.M., Guza, R.T., Elgar, S., Herbers, T.H.C., Bowen, A.J., 2006. Nonlinear generation and loss of infragravity wave energy. J. Geophys. Res. 111 (C12007). doi:10.1029/2006JC003539.
Herbers, T.H.C., Elgar, S., Guza, R.T., 1995. Generation and propagation of infragravity waves. J. Geophys. Res. 100, 24863–24872. doi:10.1029/95JC02680.
http://www.aviso.oceanobs.com.
Johannessen, O.M., Bengtsson, L., Miles, M., Kuzmina, S.I., Semenov, V., Alekseev, G.V., Nagurny, A.P., Zahkarov, V.F., Bobylev, L.P., Pettersson, L.H., Hasselmann, K., Cattle, H.P., 2004. Arctic climate change: observed and modelled temperature and sea ice variability. Tellus A 56 (4), 328–341.
LeShack, L.A., Haubrich, R.A., 1964. J. Geophys. Res. 69, 3815.
Lighthill, J., 1978. Waves in Fluids. Cambridge University Press.
Longuet-Higgins, M., Stewart, R., 1962. Radiation stress and mass transport in gravity waves, with application to surf beats. J. Fluid Mech. 13, 481–504.
Menemenlis, D., Farmer, D.M., Czipott, P.V., 1995. A note on infragravity waves in the Arctic Ocean. J. Geophys. Res. 100 (C4), 7089–7093.
Munk, W.H., Snodgrass, F.E., 1957. Measurements of southern swell at Guadeloupe Island. Deep-Sea Res. 4, 272–286.
Nagurny, A.P., Korostelev, V.G., Ivanov, V.V., Medvedchenko, E.Y., 1999. Detection and modelling of greenhouse warming in the Arctic and sub-Arctic. Report for INTAS Grant 97-1277. Arctic & Antarctic Research Institute, St. Petersburg, p. 63.
Nagurny, A.P., Korostolev, V.G., Abaza, V.P., 1994. A method for determination of effective sea ice thickness in the Arctic basin for climate monitoring. Bull. Russian Acad. Sci., Phys./Suppl. 58, 168.
Sanderson, T.J.O., 1988. Ice Mechanics - Risks to Offshore Structures. Graham & Trotman, London.
Wadhams, P., 1973. Attenuation of swell by sea ice. J. Geophys. Res. 78, 3552–3563.
Wadhams, P., 1986. The seasonal ice zone. In: Untersteiner, N. (Ed.), The Geophysics of Sea Ice. Plenum Press, New York, pp. 825–991.
Wadhams, P., Squire, V.A., Goodman, D.J., Cowan, A.M., Moore, S.C., 1988. The attenuation rates of ocean waves in the marginal ice zone. J. Geophys. Res. 93 (C6), 6799–6818.
Webb, S.C., 2007. The Earth's 'hum' is driven by ocean waves over the continental shelves. Nature 445. doi:10.1038/nature05536.
Webb, S.C., Zhang, X., Crawford, W., 1991. Infragravity waves in the deep ocean. J. Geophys. Res. 96 (C2), 2723–2736.